DOE/PC/90300--T10

RECEIVED
FEB 14 1995
OSTI

TECHNICAL PROGRESS REPORT

CONTRACT TITLE: Rapid Pressure Swing Absorption Cleanup of Post-Shift Reactor Synthesis Gas

CONTRACT NUMBER: DE-FG22-90PC90300

CONTRACT PERIOD: 9/7/90 - 8/31/93

CONTRACTOR'S NAME:
Dept. of Chemistry and Chemical Engineering
Stevens Institute of Technology
Hoboken, NJ 07030

SUBCONTRACTOR'S NAME:
Department of Chemical Engineering, Chemistry and Environmental Science
New Jersey Institute of Technology
Newark, NJ 07102

INVESTIGATORS: AT NJIT
Dr. K. K. Sirkar
Dr. S. Majumdar
Mr. S. Bhaumik

REPORT NUMBER: 10 (Final)

MASTER

Overview of Progress

A model for the separation of CO_2 from a mixture of CO_2 and N_2 using aqueous solution of diethanolamine (DEA) as a reactive absorbent has been developed for a particular type of RAPSAB cycle (mode 3). The numerical simulations of the model compare well with the experimental results.

A calibration curve for CO was made using a CTR column (Alltech Associates, Inc., Deerfield, IL). A number of experiments were carried out for the separation of CO from a mixture of CO and N_2 using a 0.4M Cu_2Cl_2 in 2M KCl solution as an absorbent. All experiments were carried out using mode 3 type of operation and a CO-N_2 mixture containing 2500 ppm CO and balance N_2. Module No. 5 was used for all experiments. The details of the module are given in Technical Progress Report No. 7.

Model Development for CO_2 Absorption in DEA Solution

A simplified model for gas absorption using an aqueous DEA solution as reactive absorbent for the separation of CO_2 from CO_2-N_2 mixture in mode 3 has been developed using Happel's (1958) free surface model. Only one fiber is considered in a unit cell of radius r_e (Figure 1) where the fiber is surrounded by the absorbent. Gas flows through the lumen of the fiber. Gas pressure drop in the fiber lumen was included in the model. The governing balance equations and boundary conditions for any species j (N_2, CO_2) in the gas and liquid phases are given below.

$$\frac{\partial C_{jg}}{\partial t} = D_{jg}\frac{\partial^2 C_{jg}}{\partial z^2} - \frac{\partial}{\partial z}\left(v_z C_{jg}\right) - \frac{4K_{jg} d_o}{d_i^2}\left(C_{jg} - C_{jg}^{\,i}\right) \qquad (1)$$

where $$C_{jg}^{\,i} = \frac{C_{jl}\big|_{r=r_o}}{H_j RT} \quad and \quad v_z = -\frac{RT d_i^2}{32\mu_g}\sum_{j=1}^{n}\frac{\partial C_{jg}}{\partial z} \qquad (2)$$

Initial Condition: at t = 0, $C_{jg} = 0$ ($0 \le z \le L$) (3)

Boundary conditions:

$$v_z C_{jg}\big|_u = v_z C_{jg}\big|_{z=0} - D_{jg}\frac{\partial C_{jg}}{\partial z}\Big|_{z=0} \quad (4); \qquad -D_{jg}\frac{\partial C_{jg}}{\partial z}\Big|_{z=L} = 0 \quad (5)$$

In the liquid phase, now, there are at least three components to be considered: N_2, CO_2, and the amine. For N_2, the mass balance equation is:

$$\frac{\partial C_{N_2l}}{\partial t} = D_{N_2l}\left(\frac{\partial^2 C_{N_2l}}{\partial r^2} + \frac{1}{r}\frac{\partial C_{N_2l}}{\partial r}\right) \qquad (6)$$

Initial condition: at t = 0, $C_{N_2l} = 0$ ($0 \le z \le L$ and $r_0 \le r \le r_e$) (7)

Boundary Conditions:

$$-D_{N_2l}\frac{\partial C_{N_2l}}{\partial r}\Big|_{r=r_o} = K_{N_2g}\left(C_{N_2g} - \frac{C_{N_2l}\big|_{r=r_o}}{H_{N_2}RT}\right) \quad (8); \qquad \frac{\partial C_{N_2l}}{\partial r}\Big|_{r=r_e} = 0 \quad (9)$$

The liquid phase mass balance for CO_2 (represented by A) is:

$$\frac{\partial C_{Al}}{\partial t} = D_{Al}\left(\frac{\partial^2 C_{Al}}{\partial r^2} + \frac{1}{r}\frac{\partial C_{Al}}{\partial r}\right) - \frac{C_{Al}\ C_{Bl}}{\dfrac{1}{k_1} + \dfrac{k_2}{k_1 k_3 C_{Bl}}} \tag{10}$$

Here diethanolamine has been represented as B.

Initial condition: $C_{Al}\ (z, r, t = 0) = 0$ (11)

Boundary Conditions:

$$-D_{Al}\frac{\partial C_{Al}}{\partial r}\Big|_{r=r_o} = K_{Ag}\left(C_{Ag} - \frac{C_{Al}|_{r=r_o}}{H_A RT}\right) \quad (12); \qquad \frac{\partial C_{Al}}{\partial r}\Big|_{r=r_e} = 0 \quad (13)$$

The corresponding mass balance equation for diethanolamine along with the initial and boundary conditions are

$$\frac{\partial C_{Bl}}{\partial t} = D_{Bl}\left(\frac{\partial^2 C_{Bl}}{\partial r^2} + \frac{1}{r}\frac{\partial C_{Bl}}{\partial r}\right) - \frac{2\ C_{Al}\ C_{Bl}}{\dfrac{1}{k_1} + \dfrac{k_2}{k_1 k_3 C_{Bl}}} \tag{14}$$

Initial condition: $C_{Bl}\ (z, r, t = 0) = C_{Bl0}$ (15)

Boundary conditions:

$$\frac{\partial C_{Bl}}{\partial r}\Big|_{r=r_o} = 0 \quad (16); \qquad \frac{\partial C_{Bl}}{\partial r}\Big|_{r=r_e} = 0 \quad (17)$$

These governing mass balance equations (6), (10), and (14) along with the corresponding initial and boundary conditions were solved numerically to find out the purified product composition at any time. They were solved using the method of lines technique to convert the PDEs (partial differential equations) into ODEs (ordinary differential equations) in time and spatial dimensions. The computer codes were written in Fortran 77 using the IMSL subroutine, DIVPAG; the program was run in the mainframe computer, VAX/VMS environment.

Calibration curve for carbon monoxide

A Varian 3700 gas chromatograph having a thermal conductivity detector (TCD) was used to calibrate the composition of the CO-containing gas using a CTR column (Alltech Associates, Inc., Deerfield, IL); this column consists actually of two concentric columns, the outer one packed with activated molecular sieve and the inner one packed with a porous polymer mixture. The outer one separates CO from CO-N_2. Calibration of CO could be done only upto 400 ppm at the lower level. The calibration curve for CO is provided in Figure 2.

Preparation of a 0.2M Cu_2Cl_2 in 2M KCl solution

The required amount of KCl was dissolved in 1 liter of DI water in a volumetric flask. Then the required amount of Cu_2Cl_2 was slowly added to KCl solution. The resulting solution should not be exposed to atmosphere because Cu_2Cl_2 could be oxidized in the presence of air. The narrow neck of the volumetric flask provided the solution with a very limited exposure to the atmosphere and thus prevented atmospheric oxidation of Cu_2Cl_2. Then the solution was stirred and slowly, concentrated hydrochloric acid was added dropwise until a clear solution was obtained. Final pH of the solution was around

2. A small amount of precipitate was observed at the bottom, but the clear supernatant was taken out and used as an absorbent in the experiment for the separation of CO from CO-N_2 mixture.

Experimental procedure

The schematic of the setup for mode 3 type of operation is given in Figure 3. All experiments for the separation of CO were carried out using mode 3 in the following manner. The feed gas was allowed to enter through the feed entrance port of the three way solenoid valve (3-WSV) (Figure 4) while the other end of the three-way solenoid valve was closed. The two-way (2-WSV) solenoid valve at the exit end of the permeator was opened simultaneously to withdraw the purified front of the mixture of gases. After some time the feed entrance port of the three-way solenoid valve as well as the two-way solenoid valve at the exit was closed; simultaneously the other end of the three-way solenoid valve was opened for vacuum desorption for a certain length of time. This completed one whole cycle of operation. The time for the absorption part of the cycle was changed in different experiments. After a certain length of operation, the purified gas mixture was injected into the GC periodically to find out the gas composition. A constant gas flow rate from the surge drum was maintained using a metering valve.

Results

The numerical model simulations have been compared with the experimental results obtained from module no. 5 and mode 3 type of operation for the separation of CO_2 from a CO_2-N_2 mixture using 19.5% DEA solution in water as an absorbent. The time duration for absorption and desorption part of the cycle in mode 3, the feed flow rate, and the purified product flow rate for all experiments are identified in Table 1 along with the purified gas composition in each case. The model simulation results have been compared with the experimental results in Figure 5 in terms of normalized high pressure exit compositions plotted against the normalized absorption time ($D_{11}t/r_e^2$). The experimental and simulated values of the purified gas flow rate for different normalized absorption times are also given in the same plot. The model results describe the data well.

We now report CO removal from CO-N_2 mixture using 0.4M Cu_2Cl_2 in 2M KCl solution as an absorbent. The time duration for absorption and desorption part of the cycle in mode 3, the feed flow rate, and the purified product flow rate for all experiments are identified in Table 2 along with the purified gas composition in each case. The feed gas flow rate was kept constant at 300 cc/min as the absorption time was changed. Module no. 5 and a feed gas mixture of 2500 ppm CO and balance N_2 were used for all experiments. As the absorption time was increased from 10 to 16 seconds, the purified product flow rate was increased. The purified product composition was at least less than 400 ppm CO and balance N_2 in each case. As mentioned earlier, the calibration of CO gas was not done below 400 ppm, so the actual composition of the purified product was not determined. However, one experiment with high absorption time would release more than 400 ppm CO in the purified product and then the purified product composition can be determined in that case even with the present calibration.

Notation

C_{Al} = concentration of species A in the liquid phase, mol/m^3

C_{Bl} = concentration of species B in the liquid phase, mol/m^3

C_{Bl0} = initial concentration of species B in the liquid phase, mol/m^3

C_{jg} = concentration of species j in the gas phase, mol/m^3

C_{N_2g} = concentration of N_2 in the gas phase, mol/m^3

D_{Al} = diffusion coefficient of species A in the liquid phase, m^2/s

D_{Bl} = diffusion coefficient of species B in the liquid phase, m^2/s

D_{jg} = diffusion coefficient of species j in the gas phase, m^2/s

D_{N_2l} = diffusion coefficient of N_2 in the liquid phase, m^2/s

d_i = inside diameter of a hollow fiber, m

d_o = outside diameter of a hollow fiber, m

H_A = solubility coefficient of gas species A in a liquid, mol/(m^3.Pa)

H_j = solubility coefficient of gas species j in a liquid, mol/(m^3.Pa)

H_{N_2} = solubility coefficient of gas N_2 in a liquid, mol/(m^3.Pa)

K_{Ag} = gas side mass transfer coefficient of species A, m/s

K_{jg} = gas side mass transfer coefficient of species j, m/s

k_{Am} = second order rate constant for the amine

k_1 = rate constant for CO_2 reaction in DEA solution, m^3/(mol.s)

k_2, k_3 = rate constant for CO_2 reaction in DEA solution

L = effective fiber length in a module, m

R = universal gas constant, $(m^3.Pa)/(mol.^\circ K)$

r = radial distance, m

r_e = equivalent radius of free surface, m

r_i = inside radius of a hollow fiber, m

r_o = outside radius of a hollow fiber, m

T = temperature, °K

t = time, s

v_z = gas velocity in fiber lumen, m/s

z = longitudinal distance, m

Greek

μ = viscosity, Pa.s

Superscript

i = interface

Subscript

g = gas phase

j = component j

l = liquid phase

u = upstream section of the hollow fiber module

Reference

Happel, J., "Viscous Flow Relative to Arrays of Cylinders," AIChE J, 5, 174 (1959).

Table 1. Experimental results for RAPSAB using DEA solution and mode 3 at a high feed gas flow rate

Experiment No.	Module No.	Absorption Time (Seconds)	Desorption Time (Seconds)	Feed Flow Rate (cc/min)	Feed Pressure (psig)	Product Outlet Composition*	Product Flow Rate (cc/min)
10.1-1	5	10	20	800	~35	CO_2: <50 ppm	52.5
10.1-2	5	12	20	800	~35	CO_2: 500 ppm	80
10.1-3	5	14	20	800	~35	CO_2: 1000 ppm	110
10.1-4	5	16	20	800	~35	CO_2: 0.2%	130
10.1-5	5	18	20	800	~35	CO_2: 0.4%	147.5
10.1-6	5	20	20	800	~35	CO_2: 0.8%	175
10.1-7	5	22	20	800	~35	CO_2: 1.2%	210
10.1-8	5	24	20	800	~35	CO_2: 2.5%	255

Feed Composition: CO_2:9.9%, N_2: 90.1%

* Balance N_2

Table 2. Experimental results for the separation of CO using Cu_2Cl_2-KCl solution$^+$, mode 3 type of operation

Experiment No.	Module No.	Absorption Time (Seconds)	Desorption Time (Seconds)	Feed Flow Rate (cc/min)	Feed Pressure (psig)	Product Outlet Composition*	Product Flow Rate (cc/min)
10-1	5	10	16	300	25	CO: <400 ppm	~17
10-2	5	12	16	300	25	CO: <400 ppm	~24
10-3	5	16	16	300	25	CO: <400 ppm	~40

+ 0.4M Cu_2Cl_2 in 2M KCl solution

* Feed Composition: CO:2500 ppm, N_2: Balance

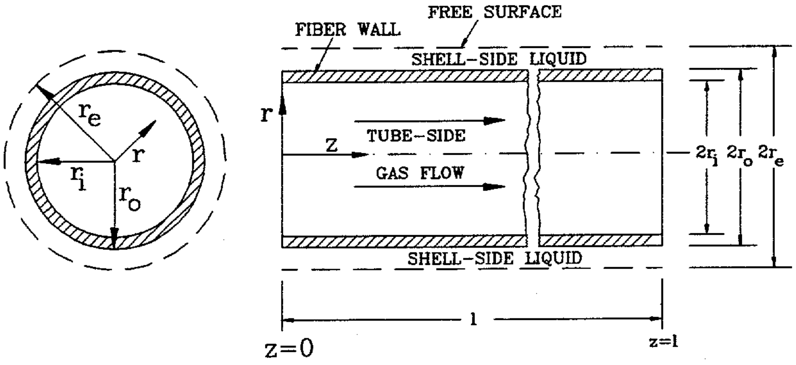

Figure 1. Schematic representation of Happel's free surface model

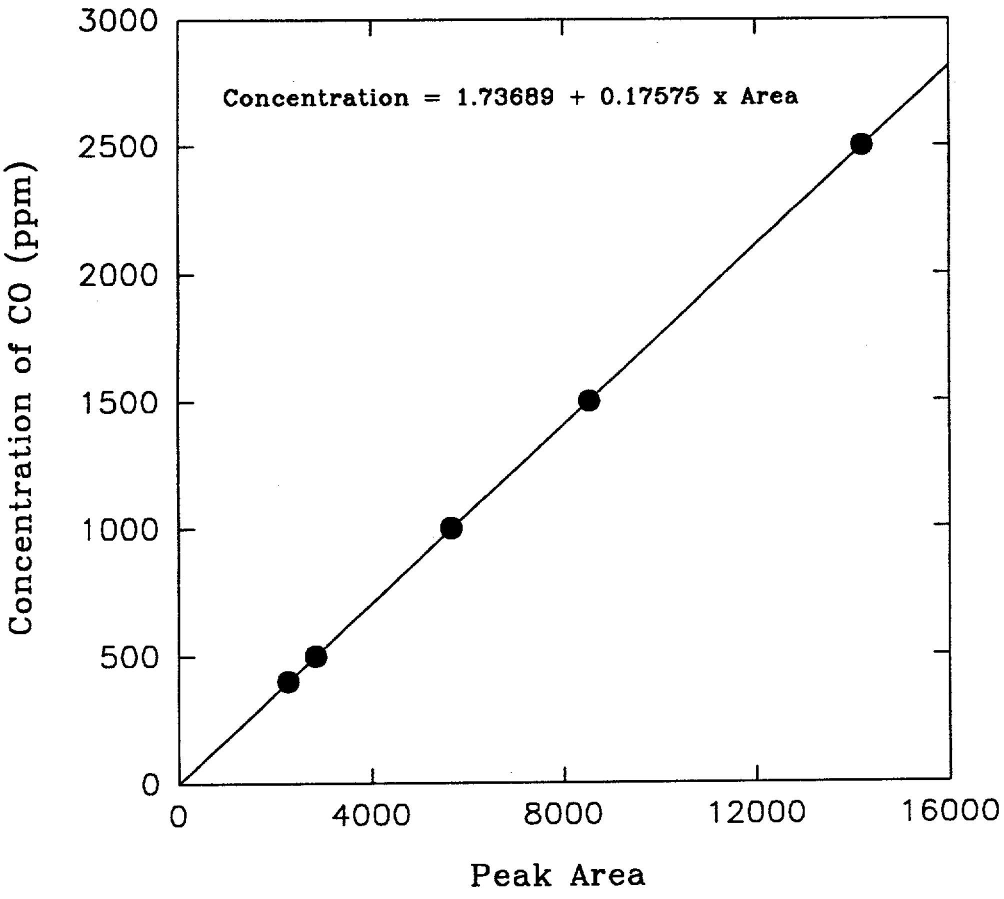

Figure 2. Calibration curve for carbon monoxide

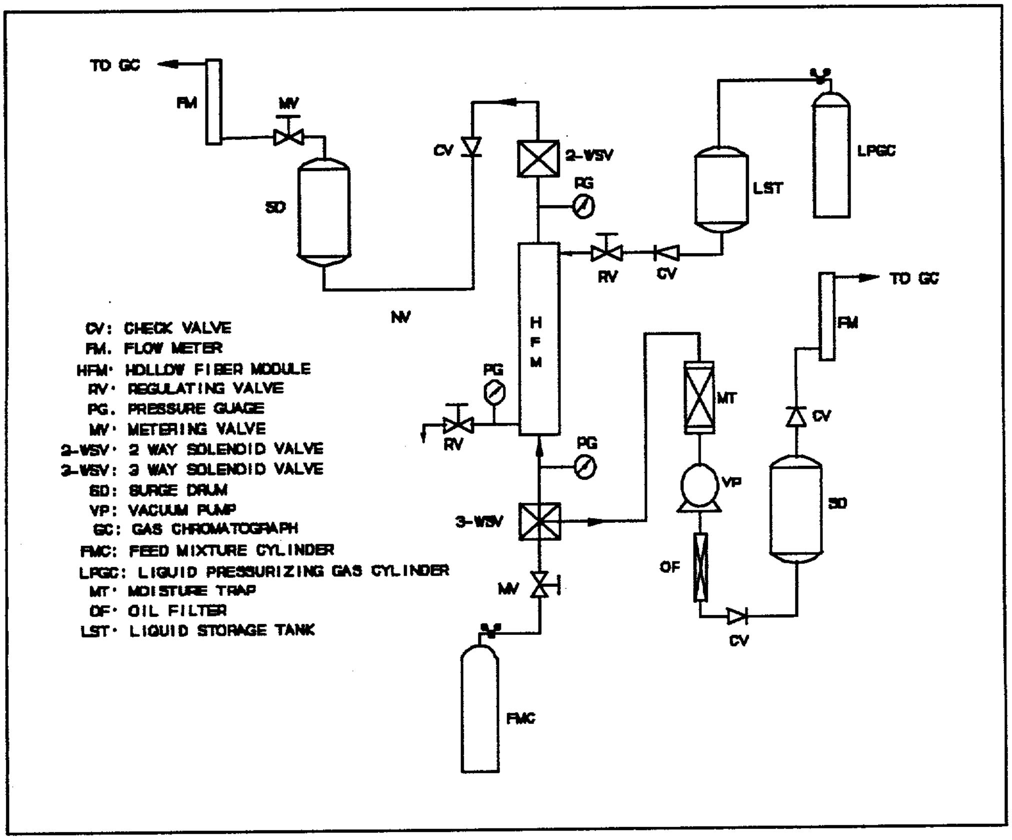

Figure 3. RAPSAB setup for Mode 3

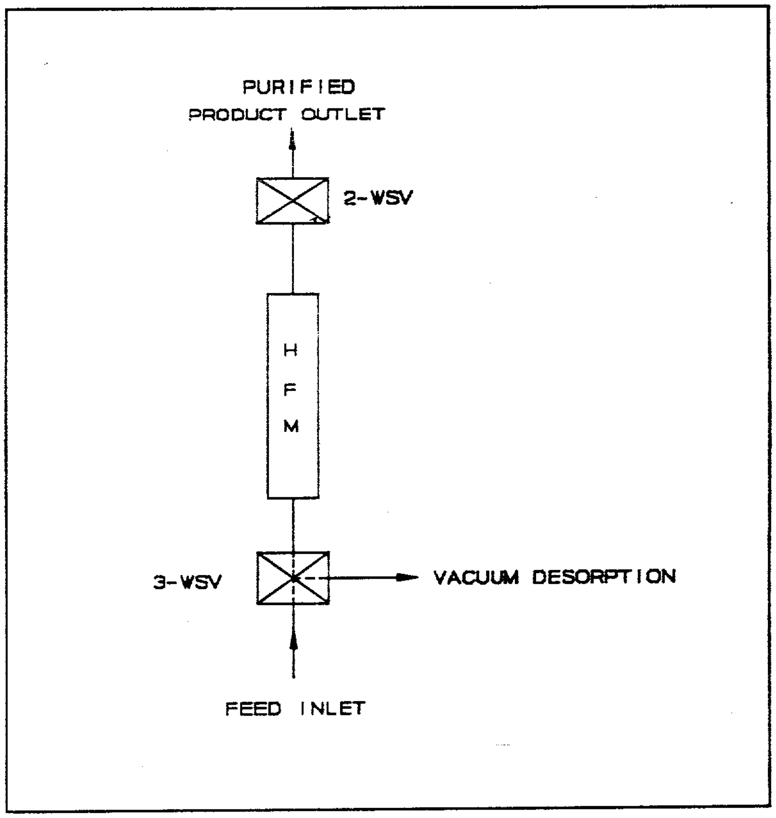

Figure 4. Solenoid valve locations in RAPSAB Apparatus for Mode 3

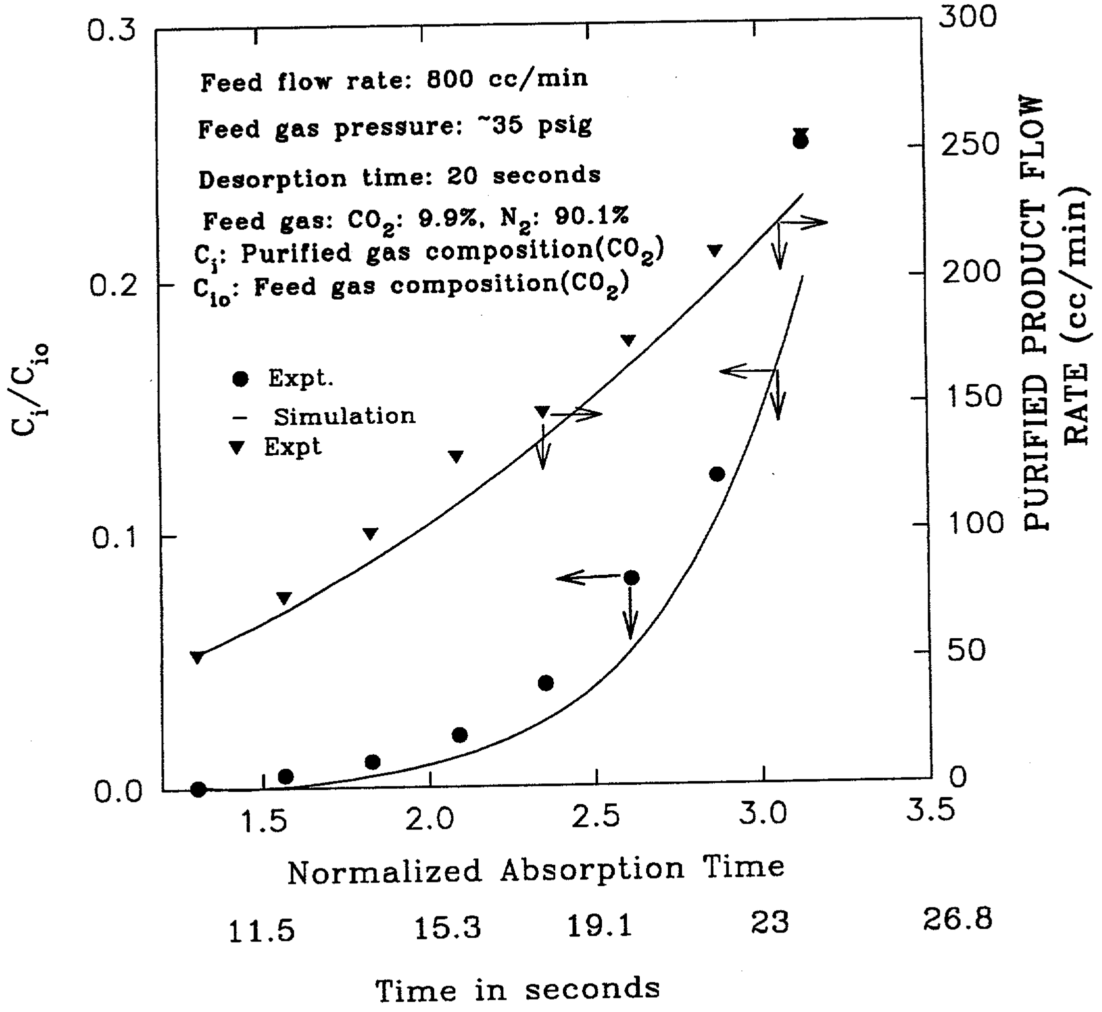

Figure 5. RAPSAB performance (mode 3) for the removal of CO_2 with DEA as an absorbent